Organic LETTERS

Letter

pubs.acs.org/OrgLett

Cooperative Dyads for Two-Photon Uncaging

Eduardo José Cueto Díaz,[†] Sébastien Picard,[†] Vincent Chevasson,[†] Jonathan Daniel,[†] Vincent Hugues,[†] Olivier Mongin,[‡] Emilie Genin,[†] and Mireille Blanchard-Desce*[,†]

[†]Univ. Bordeaux, Institut des Sciences Moléculaires, CNRS UMR 5255, 351 Cours de la Libération, F-33450 Talence Cedex, France

[‡]Institut des Sciences Chimiques de Rennes, UMR CNRS 6226, Université de Rennes 1, 35042 Rennes Cedex, France

Supporting Information

ABSTRACT: A series of dyads that combine a photolabile protecting group (PPG) 4,5-dimethoxy-2-nitrobenzyl and different bis-donor or bis-acceptor dissymmetric chromophores acting as two-photon (2P) absorbers were synthesized. Even for low energy transfer efficiency from the 2PA subunit to the uncaging one, improvement of the 2P uncaging sensitivity in the NIR is achieved as compared to isolated PPG. Moreover enhancement of the 2PA response is achieved by tuning the electronic dissymmetry of the 2PA subunit and the arrangement of the complementary subunits in the dyads.

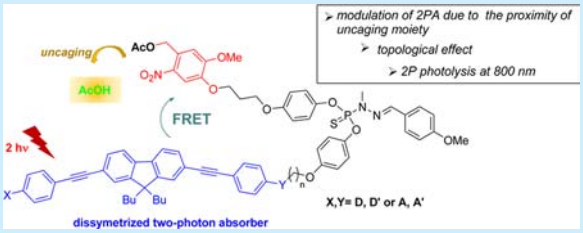

Light induced deprotection reactions have attracted significant attention, as they offer applications in various fields such as multistep organic synthesis, polymerization, volatiles release, and biology. They offer significant advantages in terms of possible external triggering with spatial and temporal control, absence of chemical additives, and compatibility with a wide range of common protecting groups. Various families of protecting groups that can be photoactivated under near-UV irradiation have been described in the literature including arylcarbonylmethyl, nitroaryl, coumarin-4-ylmethyl, arylmethyl, and metal complexes.[1] They show diverse properties in terms of photorelease kinetics, uncaging sensitivity, and dark stability which are key criteria for applications.

In recent years, two-photon excitation (2PE) has emerged as a popular tool for biological applications, as it permits performing photoactivation in the near-IR region (700−1000 nm). 2PE offers several advantages including intrinsic 3D resolution, reduced out-of focus photodamage, and improved penetration depth in tissues. However, one of the main current limitations for its widespread application in biology is the poor two-photon absorption (2PA) ability (quantified by the 2PA cross section σ_2) of most classical caging groups resulting in low 2P uncaging sensitivity (quantified by the 2P uncaging action cross section $\delta_u = \sigma_2 Q_u$, where Q_u is the uncaging quantum yield). The development of improved 2P cages displaying large δ_u values that enabled efficient 2P photorelease to be performed at nontoxic excitation intensities is thus required. Various attempts toward new uncaging moieties specifically engineered for 2PE have been conducted recently, but only very few have δ_u values over 1 GM.[2] Rather than designing new uncaging moieties, we have been interested in modular approaches where classical uncaging groups are combined with a better 2P absorber liable to transfer its excitation energy to the adjacent uncaging module. This alternative strategy was aimed at retaining critical characteristics of the uncaging unit such as dark stability, photorelease kinetics, etc. A proof of concept has been realized recently with symmetrical tandem systems having two uncaging 7-nitroindolinyl (NI) moieties grafted onto a quadrupolar 2PA module, enabling a 10-fold enhancement of 2P uncaging of glutamate derivatives as compared to MNI, leading to a δ_u of 0.7 GM at 730 nm.[3] These systems however still show a modest 2PA cross section in the biological spectral window (with a maximum of ∼40−70 GM at 710−720 nm and vanishing 2PA response at 800 nm). Based on this observation, our goal was thus the design of synergic modular systems whose 2PA responses would be significantly improved with 2PA activity maintained at a longer wavelength (typically 800 nm) to allow improved penetration depth in thick biological samples. The 4,5-dimethoxy-2-nitrobenzyl (NV) photolabile protecting group (PPG) was selected as a model PPG, as it has been used in a wide range of photoactivated systems for drug or bioactive molecules delivery[4] and has relatively good dark stability. This PPG however shows a modest 2P uncaging action cross section (δ_u = 0.03 GM at 730 nm).[2a] To confer improved 2PA responses, instead of using symmetrical quadrupolar 2PA structures built from a fluorene core[5] as done earlier,[3,6] we chose to impart *electronical dissymmetry* and designed $A_1-\pi-A_2$ or $D_1-\pi-D_2$ two-photon absorbing modules (Figure 1). The symmetry breaking was meant to relieve the symmetry interdiction of the 2P transition to the lowest excited state and thus to promote enhanced 2PA characteristics in the 700−800 nm region.[7] Based on earlier work on organic nanodots, we chose a phosphorus-based clip to control the relative positioning of 2PA and uncaging units within the dyads. This clipping module has been shown to allow cooperative increase of two-photon absorption in dipolar chromophore dimers.[8]

Received: November 13, 2014
Published: December 19, 2014

dx.doi.org/10.1021/ol5033046 | *Org. Lett.* 2015, 17, 102−105

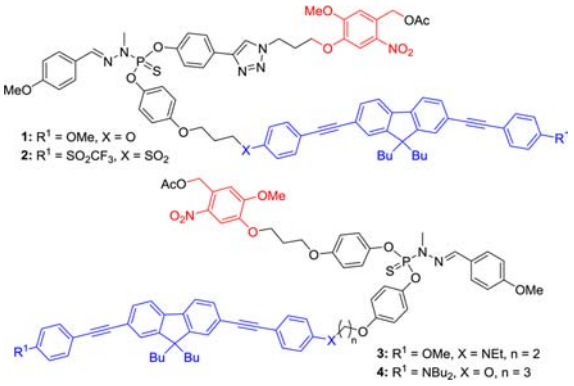

Figure 1. Design of dyads for two-photon induced acetic acid uncaging by combination of a fluorene-cored two-photon absorber (in blue) and 4,5-dimethoxy-2-nitrobenzyl (NV) uncaging moiety (in red).

The synthesis of two-photon absorbing modules **10a−d** was achieved in two steps by means of an in situ deprotection/double Sonogashira coupling of the known 2,7-diiodofluorene derivative[5] **6** with the corresponding silylated alkynes **5a−c** and **7a−d** with moderate to good yields for each step (Scheme 1). The

Scheme 1. Synthesis of Two-Photon Absorbing Modules 10a−d

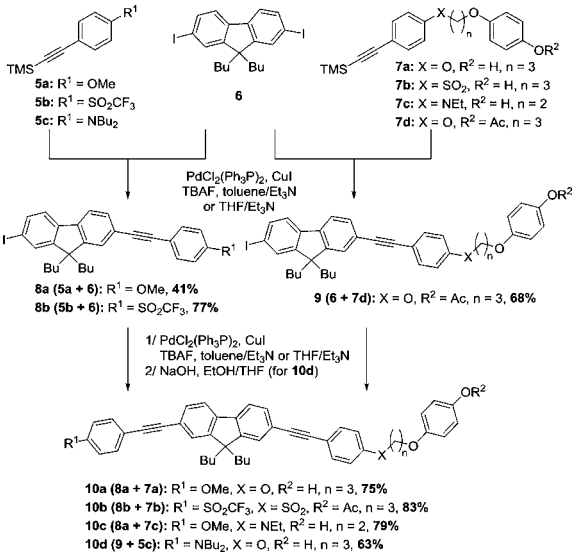

acetyl group was removed by saponification to yield the phenol moiety. The NV derivatives **11** and **13** were prepared in six steps from the same starting material, vanillin, with respectively a 29% and 33% overall yield (Scheme 2). The key steps are the introduction of the nitro group by nitration, the incorporation of the acetyl group by simple esterification, and the grafting of phenol moieties by click chemistry or by nucleophilic substitution. The experimental protocols are reported in detail in the Supporting Information (SI).

The synthesis of the targets dyads is based on highly efficient nucleophilic substitution of phenolic derivatives **10a−d**, **11**, and **13** on the known scaffold **12**[9] (Scheme 2). To obtain dyads **1−4**, we developed a one-pot procedure involving first the substitution of one Cl by a stoichiometric amount of the phenolic anion of **11** or **13**, followed by the substitution of the second Cl in the presence of the phenolic anion of **10a−d** (Scheme 2). These phenolic anions were generated by the action of cesium

Scheme 2. Synthesis of Dyads 1−4

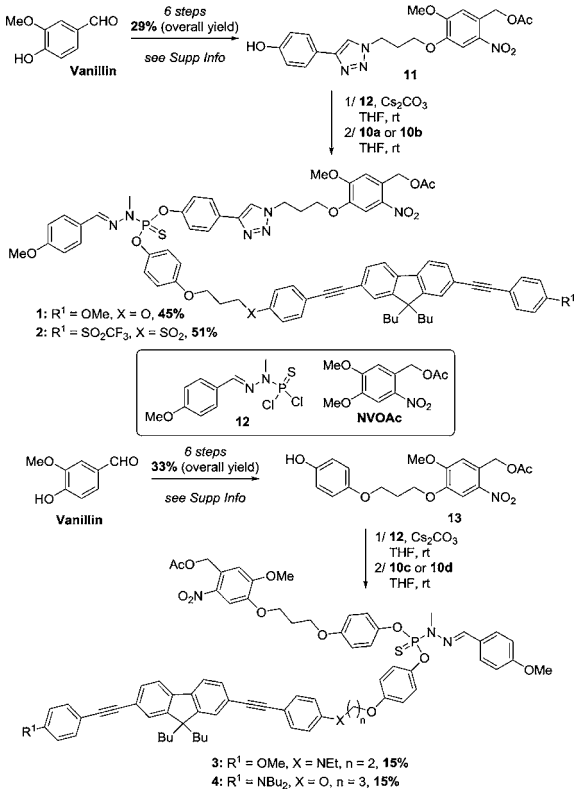

carbonate in THF in the dark. The reaction was monitored by ^{31}P and ^{1}H NMR. The first substitution was observed in ^{31}P NMR to be completed by the presence of a singlet at 69.0 ppm compared to the ^{31}P NMR signal of **12** (63.4 ppm). The dyads **1−4** were easily obtained by purification on silica gel with moderate yields. All compounds were characterized by ^{1}H, ^{13}C, ^{31}P NMR and mass spectroscopy.

The photophysical properties of dyads **1−4** and their corresponding fluorene-cored chromophoric subunits **10a−d** have been investigated, and experimental data are gathered in Table 1. Both chromophoric subunits and dyads show an intense absorption band in the near-UV, with a maximum molar extinction coefficient more than 1 order of magnitude larger than that of the isolated NV uncaging subunit. All 2P absorbing subunits (**10a−d**) display strong fluorescence emission in the violet-blue visible region (Figure 2). Increasing strength of the end groups induces a red shift of both the absorption and emission bands (Table 1). Interestingly a slight overlap between **NVOAc** absorption and 2PA subunits emission is observed (Figure 2), paving the way for energy transfer from the excited 2PA subunit to the close uncaging subunit within dyads. The overlap integral values however decrease drastically as the emission band of the 2PA subunit becomes more red-shifted (see SI). The energy transfer is thus theoretically possible in dyads **1−4**, but with markedly decreasing efficacy on going from **1** to **4**. In agreement with these expectations, the fluorescence quantum yields (except dyad **2**) and lifetimes are found to decrease in dyads **1−4** as compared to their 2PA subunits **10a−d**. The relative decrease of fluorescence is ∼40% for dyad **1** and falls to 4% for dyad **4**, following the decrease of the overlap *J* between acceptor (**NVOAc**) absorption and donor (2PA module) emission spectra. Similarly, the fluorescence lifetimes decrease by ∼40% for dyad **1** but only by 4% for dyad **4**. From these

dx.doi.org/10.1021/ol5033046 | *Org. Lett.* 2015, 17, 102−105

Table 1. Photophysical Data of Dyads 1−4 and Their Corresponding Two-Photon Absorbing Subunits 10a−d in $CHCl_3$

compd	λ_{abs}^{max} [nm]	ε^{max} [$M^{-1}\cdot cm^{-1}$]	λ_{em}^{max} [nm]	Φ_f[a]	τ_f[b] [ns]	Φ_{ET}[c]	$\varepsilon^{max}Q_u$ [$M^{-1}\cdot cm^{-1}$][d]	λ_{2PA}^{max} [nm]	σ_2^{max} [GM][e]	$\sigma_2^{max}Q_u$ [$M^{-1}\cdot cm^{-1}$]
NVOAc	341	5.9×10^3	–	–	–	–	35	730	–	0.03[f]
10a	358	7.2×10^4	384	0.70	0.66			720	30	–
1	358	9.0×10^4	383	0.45	0.40	0.38	195	730	50	0.11
10b	368	7.7×10^4	428	0.60	0.89			740	132	–
2	369	7.8×10^4	426	0.68	0.74	0.17	85	730	110	0.12
10c	368	7.8×10^4	435	0.69	0.97			750	195	–
3	367	7.6×10^4	433	0.61	0.86	0.11	50	750	160	0.10
10d	375	6.5×10^4	446	0.64	1.04			800	240	–
4	373	6.8×10^4	446	0.60	1.00	0.05	55	800	310	0.25

[a]Fluorescence quantum yield, standard: quinine in 0.5 M H_2SO_4 (Φ = 0.546). [b]Fluorescence lifetime (excitation at 370 nm). [c]Fluorescence energy transfer efficiency estimated from fluorescence quantum yields and/or lifetimes decrease in dyads. [d]One-photon uncaging values derived from comparative one-photon photolysis experiments at 365 nm, using Qu = 0.006 for NVOAc. [e]2PA cross section at λ_{2PA}^{max} derived from TPEF experiments. [f]From ref 2a.

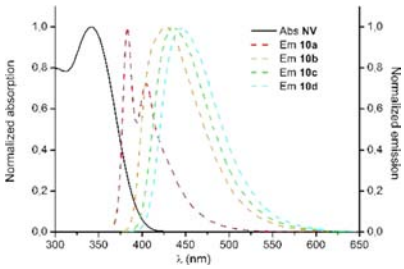

Figure 2. Absorption spectrum of veratryl uncaging module and emission spectra of 2PA modules (in $CHCl_3$).

variations, fluorescence energy transfer efficiency values could be estimated (Table 1). Whereas the energy transfer efficiency remains acceptable for dyad **1** (40%), it decreases steeply on going to dyads **3** (11%) and **4** (~5%). Since all dyads have close maximum extinction coefficients, we were thus expecting dyad **1** to have the largest one-photon uncaging sensitivity ($\varepsilon_{max}Q_u$) due to the largest FRET efficiency.

Based on these observations, the uncaging ability of dyads **1−4** was investigated by monitoring the acetic acid photorelease upon excitation at 365 nm and comparing with the uncaging behavior of **NVOAc** (see SI for experimental details). First-order kinetics was evidenced in all cases (Figure 3). As slope values are

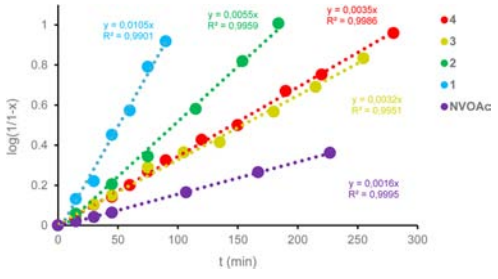

Figure 3. Kinetics of acetic acid photorelease upon excitation at 365 nm (X: conversion rate).

proportional to $\varepsilon_{365}Q_u$ values, this allowed deriving the relative Q_u values with respect to that of **NVOAc**. Using the Q_u reported for **NVOAc** in the literature,[2a] one-photon uncaging sensitivities could then be derived (Table 1). We observe that all dyads show improved one-photon uncaging sensitivity as compared to isolated **NVOAc**, and their ordering shows a similar trend to that for overlap *J* (i.e., **1** ≫ **2** ≫ **3**) indicating that FRET efficacy is indeed a critical parameter that determines dyads **1−3** uncaging sensitivity. Yet, we note that dyad **4** retains similar uncaging sensitivity ($\varepsilon^{max}Q_u$) as dyad **3**, suggesting that additional mechanisms such as photoinduced electron transfer might also be involved in the uncaging mechanism of dyad **4**.

The 2PA responses of the dyads and corresponding modules **10a−d** were investigated by performing two-photon excited fluorescence (TPEF) experiments in solution in the 700−1000 nm range using a Ti-sapphire laser delivering 140 fs pulses at a 80 MHz repetition rate. The 2PA spectra are shown in Figure 4, and 2PA maxima characteristics in the NIR region are collected in Table 1.

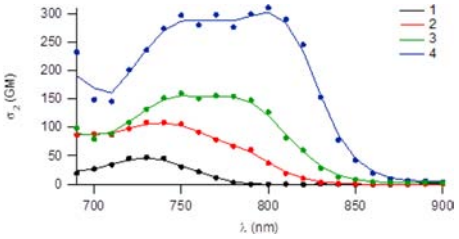

Figure 4. Two-photon absorption spectra of dyads **1−4** (in $CHCl_3$).

All chromophoric 2PA modules as well as dyads show a 2PA band located at about twice the wavelength corresponding to maximum one-photon absorption indicating that the symmetry interdiction is lowered due to the inherent dissymmetry[7,10] of both the 2PA module and dyads. As anticipated, this effect is more pronounced when the electronic dissymmetry of the 2PA chromophoric subunits is more pronounced. The 2PA band is red-shifted and the maximum 2PA cross-section (σ_2^{max}) increases significantly following the **1** → **2** → **3** → **4** and **10a** → **10d** sequences. Consequently, although modules **10a−d** and dyads **1−4** have similar 1PA cross sections, module **10d** has a σ_2^{max} value almost 1 order of magnitude larger than that of module **10a** while dyad **4** has a σ_2^{max} value which is 6 times larger than that of dyad **1** and over 300 GM. Moreover, we observe that the 2PA responses of the 2PA chromophoric subunits are significantly affected by the proximity of the uncaging unit within the dyads. This leads to a *2PA enhancement* of ~65% in the case of dyad **1** and 30% in the case of dyad **4** as compared to isolated modules **10a** and **10c** whereas a relative *decrease* of 17% is observed in the case of dyads **2** and **3**. This phenomenon can be ascribed to directional through-space electrostatic interactions within dyads. Such interactions which are known to influence the 2PA response of both dipolar[8] and quadrupolar[10] type two-photon

dx.doi.org/10.1021/ol5033046 | *Org. Lett.* 2015, 17, 102−105

absorbers are favored by the close proximity of the (dipolar) uncaging and (dissymmetrical quadrupolar) 2PA subunits within dyads. Hence, when the topology is favorable (as in dyads **1** and **4**), a positive cooperative 2PA enhancement is achieved in dyads.

Using 2PA data, we derived estimated values of the 2P uncaging action cross section (δ_u) of dyads approximating that one- and two-photon uncaging quantum yields (Q_u) are the same and using $\delta_u = Q_u\sigma_2^{max}$. As observed from Table 1, and contrary to one-photon excitation at 365 nm, all dyads show much larger two-photon uncaging sensitivity than isolated **NVOAc**, typically enhanced by a factor of 5 or 6. Quite interestingly, dyad **4** though having the lowest energy transfer efficacy and thus being the less efficient dyad for 1PP appears as a promising dyad for 2P photolysis both having the largest 2PA cross-section and being the most red-shifted chromophore allowing 2PE at 800 nm. We thus selected dyad **4** for conducting 2PP experiments at 800 nm. NMR monitoring provides evidence that 2P uncaging of acetic acid occurs upon excitation at 800 nm (Figure 5).

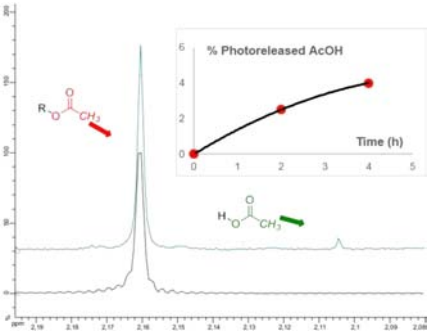

Figure 5. ^{1}H NMR spectrum (300 MHz) of **4** in $CDCl_3$ at $t = 0$ (black) and after 4 h two-photon irradiation at 800 nm (blue).

In conclusion, we have shown that the engineering of dyads that combine a dissymmetrical bis-donor chromophore that acts as the 2P absorber and a dipolar PPG can lead to synergic systems with improved 2P uncaging sensitivity at 800 nm and enhanced 2PA response. Although the reported uncaging 2P sensitivities are still moderate due to the poor uncaging quantum yield of NV and limited FRET efficacy, this opens an interesting route for the design of more efficient dyads by replacing the PPG by more efficient ones such as for instance MNI,[11] DMNPB,[12] and CDNI,[13] which have much larger uncaging quantum yields. In addition the energy transfer efficiency could be enhanced by using recently developed red-shifted PPGs that absorb in the blue visible region[14] and show large uncaging quantum yields (such as DEAC450).[14a] This would open the way to dyads with 2P uncaging sensitivity over 10 GM. In addition with the purpose of using such systems in cellular environments, water-soluble versions of these dyads will be developed.

■ ASSOCIATED CONTENT

Supporting Information

Methods, synthetic details, and NMR spectra. This material is available free of charge via the Internet at http://pubs.acs.org.

■ AUTHOR INFORMATION

Corresponding Author

*E-mail: mireille.blanchard-desce@u-bordeaux.fr.

Notes

The authors declare no competing financial interest.

■ ACKNOWLEDGMENTS

This work was supported by funding from the European Community's Seventh Framework Program under TOPBIO Project-Grant Agreement No. 264362. We also acknowledge financial support from Agence Nationale pour la Recherche (Grant 2010 ANR-10-BLAN-1436). M.B.D. thanks the Conseil Régional d'Aquitaine for generous funding (Chaire d'Accueil grant and fellowship to V.H.). The authors are grateful to Jean-Pierre Majoral and Anne-Marie Caminade (LCC UPR 8241, Toulouse, France) for the generous gift of MMH-$PSCl_2$.

■ REFERENCES

(1) Klán, P.; Šolomek, T.; Bochet, C. G.; Blanc, A.; Givens, R.; Rubina, M.; Popik, V.; Kostikov, A.; Wirz, J. *Chem. Rev.* **2013**, *113*, 119 and references cited therein.

(2) (a) Furuta, T.; Wang, S. S.-H.; Dantzker, J. L.; Dore, T. M.; Bybee, W. J.; Callaway, E. M.; Denk, W.; Tsien, R. Y. *Proc. Natl. Acad. Sci. U.S.A.* **1999**, *96*, 1193. (b) Gagey, N.; Neveu, P.; Benbrahim, C.; Goetz, B.; Aujard, I.; Baudin, J.-B.; Jullien, J. *J. Am. Chem. Soc.* **2007**, *129*, 9986. (c) Donato, L.; Mourot, A.; Davenport, C. M.; Herbivo, C.; Warther, D.; Léonard, J.; Bolze, F.; Nicoud, J.-F.; Kramer, R. H.; Goeldner, M.; Specht, A. *Angew. Chem., Int. Ed.* **2012**, *51*, 1840 and references cited therein. (d) Bort, G.; Gallavardin, T.; Ogden, D.; Dalko, P. I. *Angew. Chem., Int. Ed.* **2013**, *52*, 4526 and references cited therein.

(3) Picard, S.; Cueto-Diaz, E.; Genin, E.; Clermont, G.; Acher, F.; Ogden, D.; Blanchard-Desce, M. *Chem. Commun.* **2013**, *49*, 10805.

(4) (a) Kantevari, S.; Hoang, C. J.; Ogrodnik, J.; Egger, M.; Niggli, E.; Ellis-Davies, G. C. R. *ChemBioChem.* **2006**, *7*, 174. (b) Tang, H.; Kim, K. H.; Zheng, N.; Song, Z.; Gabrielson, N. P.; Lu, H.; Cheng, J. *Angew. Chem., Int. Ed.* **2013**, *52*, 9182.

(5) Mongin, O.; Porres, L.; Charlot, M.; Katan, C.; Blanchard-Desce, M. *Chem.—Eur. J.* **2007**, *13*, 1481.

(6) Gug, S.; Bolze, F.; Specht, A.; Bourgogne, C.; Goeldner, M.; Nicoud, J.-F. *Angew. Chem., Int. Ed.* **2008**, *47*, 9525.

(7) Katan, C.; Charlot, M.; Mongin, O.; Le Droumaguet, C.; Jouikov, V.; Terenziani, F.; Badaeva, E.; Tretiak, S.; Blanchard-Desce, M. *J. Phys. Chem. B* **2010**, *114*, 3152.

(8) Robin, A.-C.; Parthasarathy, V.; Pla-Quintana, A.; Mongin, O.; Terenziani, F.; Caminade, A.-M.; Majoral, J.-P.; Blanchard-Desce, M. *SPIE Proc.* **2010**, *7774*, 77740N/1.

(9) Keller, M.; Ianchuk, M.; Ladeira, S.; Taillefer, M.; Caminade, A.-M.; Majoral, J.-P.; Ouali, A. *Eur. J. Org. Chem.* **2012**, *5*, 1056.

(10) Rouxel, C.; Charlot, M.; Mongin, O.; Tathavarathy, R. K.; Caminade, A.-M.; Majoral, J.-P.; Blanchard-Desce, M. *Chem.—Eur. J.* **2012**, *18*, 16450.

(11) (a) Papageorgiou, G.; Corrie, J. E. T. *Tetrahedron* **2000**, *56*, 8197. (b) Matsuzaki, M.; Ellis-Davies, G. C. R.; Nemoto, T.; Miyashita, Y.; Lino, M.; Kasai, H. *Nat. Neurosci.* **2001**, *4*, 1086.

(12) Specht, A.; Thomann, J. S.; Alarcon, K.; Ogden, D.; Furuta, T.; Kurakawa, Y.; Goeldner, M. *ChemBioChem* **2006**, *7*, 1690.

(13) Ellis-Davies, G. C. R.; Matsuzaki, M.; Paukert, M.; Kasai, H.; Bergles, D. E. *J. Neurosci.* **2007**, *27*, 6601.

(14) (a) Olson, J. P.; Kwon, H.-B.; Takasaki, K. T.; Chiu, C. Q.; Higley, M. J.; Sabatini, B. L.; Ellis-Davies, G. C. R. *J. Am. Chem. Soc.* **2013**, *135*, 5954. (b) Fournier, L.; Gauron, C.; Xu, L.; Aujard, I.; Le Saux, T.; Gagey-Eilstein, N.; Maurin, S.; Dubruille, S.; Baudin, J.-B.; Bensimon, D.; Volovitch, M.; Vriz, S.; Jullien, L. *ACS Chem. Biol.* **2013**, *8*, 1528.